

Specific heat in the spin model for $\text{Nd}_{2-x}\text{Ce}_x\text{CuO}_4$

Jan Bała

Institute of Physics, Jagellonian University, Reymonta 4, PL-30059 Kraków, Poland

(Received 26 September 1997; revised manuscript received 30 December 1997)

The spin interactions in $\text{Nd}_{2-x}\text{Ce}_x\text{CuO}_4$ are described by an extended Heisenberg model and treated in the spin-wave formalism including magnon-magnon scattering. The effect of doping in the model was mimicked by additional frustrating interactions in the CuO_2 planes. In the limit of strong Cu-Cu correlations, increasing frustration leads to a drastic increase in the low-temperature specific heat anomaly. The spin dynamics was treated beyond linear spin-wave order and the model was solved self-consistently. [S0163-1829(98)03422-5]

I. INTRODUCTION

The discovery of an extreme enhancement of the low-temperature specific heat in an electron-doped $\text{Nd}_{2-x}\text{Ce}_x\text{CuO}_4$ (NCCO) compound¹ renewed the interest in the superconducting materials containing magnetic rare earth ions.² In some respect these compounds are similar to hole-doped high-temperature superconducting oxides (HTSO's) (e.g., La_2CuO_4). Their three-dimensional (3D) long range order (LRO) originates from Cu^{2+} ($S=1/2$) spins with very large intraplanar exchange, greater than 100 meV, and very small interplanar exchange, less than 10^{-2} meV. However, La^{+3} ions are nonmagnetic, whereas electron-doped systems have localized moments that can order leading to a series of complicated reorientation transitions.^{3,4}

Inelastic neutron scattering experiments show that low-energy Nd excitations have energies below 0.8 meV,⁵ while the Cu excitations appear for energies greater than 10 meV (at $T < 10$ K).⁶ At low temperatures ($T < 2$ K) Nd^{+3} 4f moments order by an exchange coupling to the Cu^{+2} spins leading to a complex noncollinear structure.⁷ At small doping ($x \approx 0.1$), where the antiferromagnetic (AF) LRO of Cu moments still exists, one can observe a linear in temperature specific heat C_p with a γ coefficient ($\gamma = C_p/kT$) increasing very rapidly up to ~ 4 J/mole K^2 , indicating heavy-fermion-like behavior,¹ although not originating from Kondo-type electron exchange. This intriguing behavior was investigated in a model for strongly correlated conduction electrons hybridizing with neodymium 4f states⁸ and then by numerical diagonalization of finite clusters,⁹ a stochastic approach,¹⁰ using pseudospin models,^{11,12} and renormalization-group methods.¹³

In undoped case these materials are AF charge-transfer insulators with one hole per Cu site while with increasing doping the AF LRO disappears rapidly¹⁴ and in a narrow doping range² ($0.13 < x < 0.18$) a superconducting state is stabilized. Such a fast destruction of the AF ordered phase by doping follows from the competition between the Cu-Cu superexchange and the Kondo interactions between the doped oxygen holes and the Cu spins.¹⁵ In the doped system the oxygen holes in the CuO_2 planes modify the exchange interactions between neighboring Cu spins and induce additional spin fluctuations due to their hopping over the oxygen orbitals, which leads to a considerable frustration of the AF interactions in the planes. An explicit treatment of hole-hole

interactions is complicated. Hence we shall study instead an effective Heisenberg ($S=1/2$) model, with the effect of finite doping simulated by the frustration of AF interactions in copper planes.¹⁶ However, one has to be aware of the fact that the behavior of the doped holes in HTSO's is too complicated to be described by simple spin models to its full extent.¹⁷

II. MODEL HAMILTONIAN

We start from an extended Heisenberg model including the most important magnetic interactions in the compound. Magnetic moments of Cu^{+3} and Nd^{+3} ions are $\sim 0.4\mu_B$ and $\sim 1.3\mu_B$ at $T=0.4$ K,³ respectively. Here they are described by $S=1/2$ spins since the crystal-field ground state is known to be a singlet.^{5,18} Thus our Hamiltonian is

$$H = J \sum_{\langle ij \rangle} \mathbf{S}_i^d \mathbf{S}_j^d + J' \sum_{\langle ij \rangle} \mathbf{S}_i^d \mathbf{S}_j^f + J'' \sum_{\langle ij \rangle_{IP}} \mathbf{S}_i^d \mathbf{S}_j^d + \alpha J \sum_{\langle\langle ij \rangle\rangle} \mathbf{S}_i^d \mathbf{S}_j^d, \quad (2.1)$$

where the first two terms describe the AF ($J, J' > 0$) interactions between the Cu-Cu and Cu-Nd nearest neighbors ($\langle ij \rangle$), respectively. The next term stands for a small Cu-Cu interplane ($\langle ij \rangle_{IP}$) AF coupling ($J'' > 0$) making the model 3D (see Fig. 1) and the calculations at nonzero temperatures possible.¹⁹ Finally, the last term describes the frustrating AF interaction with the coefficient α standing for the ratio of the copper next-nearest-neighbor ($\langle\langle ij \rangle\rangle$) AF interaction to the superexchange J . The presence of magnetic interactions me-

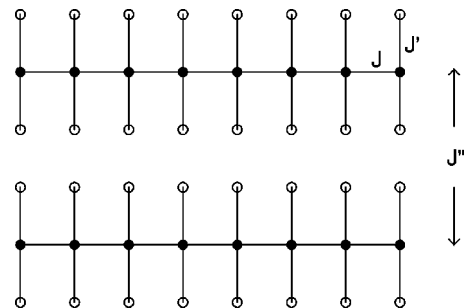


FIG. 1. Schematic structure of NCCO considered in our model. ● and ○ represent Cu and Nd sites, respectively.

diated through the copper-oxygen layers is significant as these layers are involved in superconductivity in the electron-doped compounds.

The model (2.1) with $J' = J'' = 0$ recently has been a subject of intensive theoretical studies^{20–32} and it is well established that LRO exists at $T=0$ and $\alpha=0$ while increasing α destabilizes the AF state. Exact results on finite lattices indicate that for $\alpha_{crit} \approx 0.4$ (Refs. 20–22) the conventional collinear AF LRO breaks down and including inhomogeneities simulating doping this critical frustration can be reduced even to $\alpha \approx 0.15$.²² On the other hand, spin-wave calculations show that the Néel state becomes unstable around $\alpha_{crit} \approx 0.5$.^{23–25} Furthermore, a systematic $1/N$ expansion,²⁶ self-consistent spin-wave theory²⁷, and Schwinger boson mean-field theory²⁸ found the stability of the Néel state enhanced by quantum fluctuations leading to α_{crit} larger than 0.5. In the region of strong frustration ($\alpha \approx 0.5$) several types of states have been considered: a quantum spin liquid,^{22,23,29} a short-range resonating valence bond state,^{23,30} and dimerized^{21,24,26,31} or chiral^{21,22,32} states.

To simplify the notation (and reduce the number of spin operators in our model) we have made a rotation of spins on one of the sublattices B by 180° about the S^x axis and deal with the *ferromagnetic* Néel state and spin operators transformed as³³

$$S_i^{\xi, \pm} \rightarrow S_i^{\xi, \mp}, \quad S_i^{\xi, z} \rightarrow -S_i^{\xi, z}, \quad i \in B, \quad (2.2)$$

where $\xi = d, f, f'$ describes three different sites (one Cu and two Nd) in our unit cell. Next we introduce the Bose operators d_i, f_i, f'_i by means of the Holstein-Primakoff transformation, which for \mathbf{S}_i^d spin operators has the form

$$\begin{aligned} S_i^{d,+} &= (2S)^{1/2} d_i^\dagger \left(1 - \frac{d_i^\dagger d_i}{2S} \right)^{1/2}, \\ S_i^{d,-} &= (2S)^{1/2} \left(1 - \frac{d_i^\dagger d_i}{2S} \right)^{1/2} d_i, \\ S_i^{d,z} &= S - d_i^\dagger d_i \end{aligned} \quad (2.3)$$

and is expressed in the same way for \mathbf{S}_i^f and $\mathbf{S}_i^{f'}$ spin operators. In Fourier space, including the higher-order $\sim 1/2S$ terms in the expansion of spin operators [Eq. (2.3)], our Hamiltonian has the form

$$H = H_d + H_f + H_{df}, \quad (2.4)$$

where

$$\begin{aligned} H_d &= \sum_{\mathbf{k}} [A_{\mathbf{k}}^d (d_{\mathbf{k}}^\dagger d_{\mathbf{k}} + d_{-\mathbf{k}}^\dagger d_{-\mathbf{k}}) + B_{\mathbf{k}}^d (d_{\mathbf{k}}^\dagger d_{-\mathbf{k}}^\dagger + d_{\mathbf{k}} d_{-\mathbf{k}})], \\ H_f &= A^f \sum_{\mathbf{k}} (f_{\mathbf{k}}^\dagger f_{\mathbf{k}} + f_{-\mathbf{k}}^\dagger f_{-\mathbf{k}} + f_{\mathbf{k}}'^\dagger f_{\mathbf{k}}' + f_{-\mathbf{k}}'^\dagger f_{-\mathbf{k}}'), \quad (2.5) \\ H_{df} &= A^{df} \sum_{\mathbf{k}} [(d_{\mathbf{k}}^\dagger f_{-\mathbf{k}}^\dagger + d_{\mathbf{k}} f_{-\mathbf{k}}) \cos(k_z b) \\ &\quad + (d_{\mathbf{k}}^\dagger f_{-\mathbf{k}}'^\dagger + d_{\mathbf{k}} f_{-\mathbf{k}}') \sin(k_z b)], \end{aligned}$$

with

$$\begin{aligned} A_{\mathbf{k}}^d &= \frac{zS}{2} \left[\left(J + \frac{1}{2} J'' \right) (1 - n_d) + \frac{1}{2} J_{\parallel}' \left(1 - \frac{n_f + n_{f'}}{2} \right) \right. \\ &\quad \left. + \alpha J (1 - n_d) (\gamma_{\mathbf{k}} - 1) \right], \\ B_{\mathbf{k}}^d &= \frac{zS}{2} \left[J (1 - n_d) \gamma_{\mathbf{k}} + \frac{1}{2} J'' (1 - n_d) \cos(k_z c) \right], \end{aligned} \quad (2.6)$$

$$A^f = \frac{zS}{8} J_{\parallel}' (1 - n_d),$$

$$A^{df} = \frac{\sqrt{2}zS}{4} J_{\perp}' \left(1 - \frac{2n_d + n_f + n_{f'}}{4} \right).$$

Here $\gamma_{\mathbf{k}} = \frac{1}{2} [\cos(ak_x) + \cos(ak_y)]$, $\gamma_{\mathbf{k}}' = \cos(ak_x) \cos(ak_y)$, and $z=4$ is the in-plane coordination number. The lattice parameters a , b , and c stand for the Cu-Cu in-plane, Cu-Nd, and Cu-Cu interplane nearest-neighbor distances, respectively. J_{\parallel}' and J_{\perp}' represent the exchange J' parallel and perpendicular to the z axis, respectively, and the quantities $n_d, n_f, n_{f'}$ are renormalizations of parameters for the model considered beyond the linear-spin-wave approximation (LSWA). In Sec. III we consider the limit $J_{\perp}' = 0$ giving $H_{df} = 0$ and in Sec. IV, where $J_{\perp}' = J_{\parallel}' \neq 0$, we make a simplifying approximation to the H_{df} term.

The specific heat is calculated from the total energy of excited magnons at the temperature T , which is given by

$$\begin{aligned} E(T) &= \frac{1}{N} \sum_{\mathbf{k}, i=d, f, f'} \omega^i(\mathbf{k}, T) \left[N_i(\mathbf{k}, T) + \frac{1}{2} \right] \\ &\quad - \frac{1}{2} \left(\frac{1}{N} \sum_{\mathbf{k}} A_{\mathbf{k}}^d + 2A^f \right), \end{aligned} \quad (2.7)$$

where $N_i(\mathbf{k}, T) = \{\exp[\omega^i(\mathbf{k}, T)/kT] - 1\}^{-1}$ is the Bose distribution function with magnon energies $\omega^i(\mathbf{k}, T)$. Our unit cell consists of three sites (one Cu and two Nd) and we will have three different magnon branches. The spin susceptibility perpendicular to the magnetization axis can be calculated in the same way as for a simple Heisenberg model³⁴ and expressed as

$$\chi_{\perp} = \frac{N(g\mu_B)^2}{z} \frac{12A^f(A^f - A^{df}) + 8A^f(A_{\mathbf{0}}^d + B_{\mathbf{0}}^d) + (A^{df})^2}{A^f[4A^f(A_{\mathbf{0}}^d + B_{\mathbf{0}}^d) - (A^{df})^2]}. \quad (2.8)$$

All the numerical calculations were made on a $100 \times 100 \times 100$ \mathbf{k} lattice leading to the results almost indistinguishable from the ones for $200 \times 200 \times 200$ points. The self-consistency has been carried out until the renormalization factors ($n_d, n_f, n_{f'}$) change less than 0.001% on each loop.

The model is considered only below the Nd^{3+} ordering transition ($T \sim 2$ K).³⁵ At higher temperatures the Nd ions have only moments induced by copper ions participating in the 3D LRO below the Cu^{2+} Néel temperature. In the classical limit the AF Néel state changes from two sublattices to four sublattices at $\alpha = 0.5$. Here we have considered only $0 \leq \alpha \leq 0.4$ representing the situation in a doped compound

with AF LRO still present ($x < 0.13$). This compound has the simplest crystal structure of all the cuprate superconductors with no apical oxygen.^{3,11} Therefore, our model consists of only three-plane subsystems (see Fig. 1) communicating with each other through a small exchange element J'' . In a real compound the energetic scales for the Cu-Cu intraplane exchange, the Nd-like magnetic excitations, and interplane Cu-Cu exchange are ~ 100 meV, ~ 1 meV, and $\sim 10^{-1} - 10^{-2}$ meV, respectively.^{5,12,36,37} This justifies the choice of $J/J' = 100$ and $J''/J' = 0.1$ as a realistic parameters set (with J' adopted as the energy unit). Moreover, we have assumed the lattice ratio $a/c = 3$ in agreement with NCCO lattice parameters ($a = 3.962$ Å and $c = 12.21$ Å at 300 K).^{3,35}

III. ISING LIMIT ($J'_\perp = 0$)

In this section we consider the case when Nd-Cu interactions are Ising-like ($J'_\perp = 0$). As it is shown below, even in this simplified case it is possible to explain the anomaly in the specific heat observed experimentally.¹ The Hamiltonian (2.5) is diagonalized by the Bogoliubov transformation

$$\begin{aligned} \alpha_{\mathbf{k}} &= u_{\mathbf{k}} d_{\mathbf{k}} - v_{\mathbf{k}} d_{-\mathbf{k}}^\dagger, \\ u_{\mathbf{k}} &= \left[\frac{1 + (1 - x_{\mathbf{k}}^2)^{1/2}}{2(1 - x_{\mathbf{k}}^2)^{1/2}} \right]^{1/2}, \\ v_{\mathbf{k}} &= -\text{sgn}(B_{\mathbf{k}}^d) \left[\frac{1 - (1 - x_{\mathbf{k}}^2)^{1/2}}{2(1 - x_{\mathbf{k}}^2)^{1/2}} \right]^{1/2}, \end{aligned} \quad (3.1)$$

where $x_{\mathbf{k}} = B_{\mathbf{k}}^d / A_{\mathbf{k}}^d$, giving

$$H = \sum_{\mathbf{k}} \omega^d(\mathbf{k}, T) \alpha_{\mathbf{k}}^\dagger \alpha_{\mathbf{k}} + \omega^f(T) \sum_{\mathbf{k}} (f_{\mathbf{k}}^\dagger f_{\mathbf{k}} + f_{\mathbf{k}}'^\dagger f_{\mathbf{k}}'), \quad (3.2)$$

with $\omega^d(\mathbf{k}, T) = 2\sqrt{(A_{\mathbf{k}}^d)^2 - (B_{\mathbf{k}}^d)^2}$ and $\omega^f(T) = 2A^f$. The model has to be solved self-consistently with the renormalizations of parameters

$$\begin{aligned} n_d &= \frac{1}{N} \sum_{\mathbf{k}} (u_{\mathbf{k}}^2 + v_{\mathbf{k}}^2) N_d(\mathbf{k}, T) + \frac{1}{N} \sum_{\mathbf{k}} v_{\mathbf{k}}^2, \\ n_f &= n_{f'} = \frac{1}{N} \sum_{\mathbf{k}} N_f(\mathbf{k}, T). \end{aligned} \quad (3.3)$$

The respective magnetic moments are $M_\xi = S - n_\xi$ with $\xi = d, f, f'$.

In Fig. 2 we have presented the zero-temperature dispersions of copper and neodymium spin waves at different frustration levels. Both Nd-like branches are momentum independent and soften with increasing frustration. On the other hand, for the Cu magnon mode softening takes place only for $\mathbf{k} \neq 0$ and is the strongest at large momenta [see Fig. 2(a)]. Assuming $J = 0.13$ eV, the copper-spin-wave gap $\Delta_d \sim \sqrt{JJ'}$ is about 15 meV, in reasonable agreement with the experimental value, greater than 10 meV.⁶ This gap sets the scale of the effective copper-neodymium interactions as in the limit $J' \rightarrow 0$ we have $\Delta_d = 0$. For realistic parameters $\Delta_d \gg kT$ and the copper contribution to the total energy of the system comes mainly from the $1/2N \sum_{\mathbf{k}} [\omega^d(\mathbf{k}, T) - A_{\mathbf{k}}^d]$ term

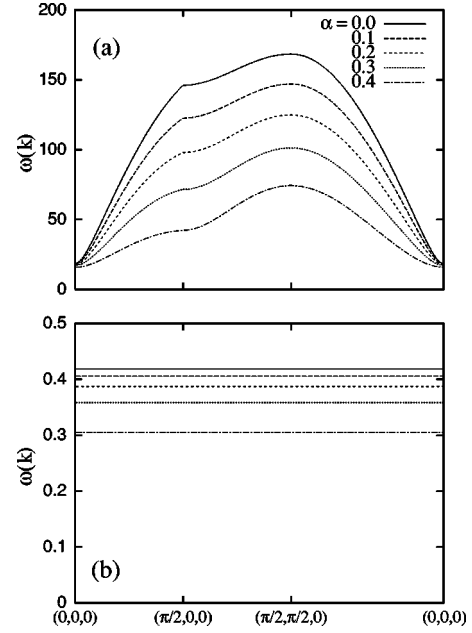


FIG. 2. Dispersions of (a) Cu and (b) Nd-like spin waves for different frustrations α in the model found in the Ising limit $J'_\perp = 0$ for the realistic parameters of NCCO at $T = 0$.

[see Eq. (2.7)]. As it will be shown below, going beyond the LSWA, this contribution can drastically alter the γ coefficient in the strongly frustrated model.

Next we analyze the effect of frustration (mimicking doping in the compound) on the γ coefficient for realistic parameters. For $kT < 0.1J'$ one can see the usual exponential increase in γ , while for large T a linear specific heat stabilizes with a rapidly increasing value for $\alpha > 0.3$ [Fig. 3(a)]

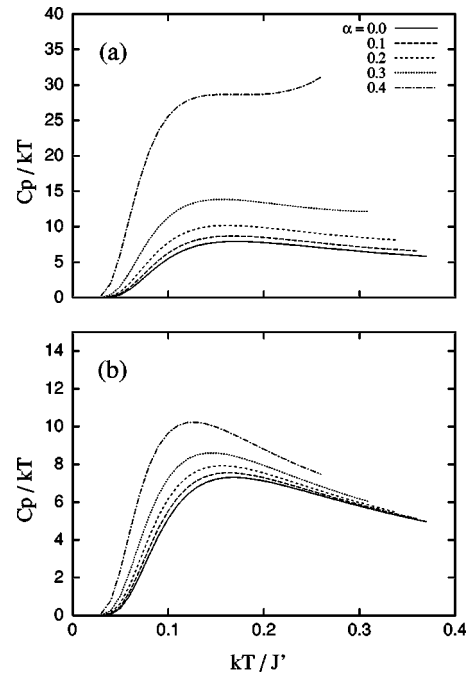


FIG. 3. Temperature dependence of $\gamma = C_p/kT$ for different frustrations α found in the Ising limit $J'_\perp = 0$ (a) with and (b) without magnon-magnon interactions, calculated for realistic parameters of NCCO.

and when higher-order terms in the Holstein-Primakoff expansion are included. On the other hand, when the problem is treated in the LSWA the magnon dispersions are temperature independent and the copper mode practically do not contribute to the specific heat ($\Delta_d \gg kT$). Therefore, the changes in γ are only due to softening of Nd modes [see Fig. 3(b)]. This indicates that the Cu-Nd magnon-magnon scattering dominates the magnon dynamics leading to heavy-fermion-like behavior.

We have investigated the temperature dependence of magnetic moments at different frustration levels. At $T=0$ the Nd magnetic moment is always $0.5\mu_B$, while the Cu one decreases from $\sim 0.34\mu_B$ to $\sim 0.11\mu_B$ when α increases from 0 to 0.4, respectively (see Fig. 4). This corresponds to decreasing Cu Néel temperature with doping. For $\alpha > \alpha_{crit} \approx 0.45$ the AF Néel ground state becomes unstable in our model. This instability occurs for a similar value of α as in the 2D frustrated Heisenberg model using spin-wave formalism.^{25,24,23} The character of the γ coefficient starts to change dramatically at $\alpha \approx 0.3$ when the copper magnetic moment reduction is $M_d(\alpha=0.3)/M_d(\alpha=0) \approx 0.7$, in agreement with the experimentally observed ratio.¹² In nonfrustrated model the Cu magnetic moment changes only by $\Delta M_d \approx 0.01\mu_B$ (when M_f changes from $0.5\mu_B$ to 0), while for $\alpha=0.4$ we have $\Delta M_d \approx 0.1\mu_B$ [see Fig. 4(a)], explaining so active a role played by the strongly correlated moments contributing to the specific heat. In all cases we have found nondiverging spin deviations.

We have also investigated to what extent this sharp increase in the γ coefficient is influenced by changes in the parameters of the model. One can see that γ slowly decreases with increasing Cu-Cu interplane interaction J'' [compare Fig. 3(a) with Figs. 5(a) and 5(b)], but a rapid reduction takes place with decreasing Cu-Cu intraplane exchange J [see Figs. 5(c) and 5(d)]. At $J/J' = 1$, when higher-order terms are negligible, we have an almost- α -independent γ coefficient. Thus one can see that strongly correlated copper spins ($J \gg J'$) are the main factor determining the rapid increase in the γ coefficient in our spin model.

IV. HEISENBERG LIMIT ($J'_\perp = J'_\parallel$)

In this section the spin model is considered in the limit where the Nd-Cu interactions have the Heisenberg form.

$$[H(\mathbf{k})] = \begin{bmatrix} \omega^d(\mathbf{k}) & 2A^{df}v_{\mathbf{k}}\cos(k_z b) & 2A^{df}v_{\mathbf{k}}\sin(k_z b) \\ 2A^{df}v_{\mathbf{k}}\cos(k_z b) & 2A^f & 0 \\ 2A^{df}v_{\mathbf{k}}\sin(k_z b) & 0 & 2A^f \end{bmatrix}. \quad (4.4)$$

Such an approximation works very well in the $J \gg J'$ limit (compare solid and dashed lines in Fig. 6) giving practically linear dispersion of the lowest mode for $\mathbf{k} \rightarrow 0$ (Fig. 7).

Although the rotational invariance has been lost and at the $\mathbf{k}=0$ point the $\sim 0.02J'$ gap opens, it can only affect the low-temperature behavior with $kT < 0.02J'$ (exponential increase of γ in this range of temperatures), which is of minor

interest here. At higher temperatures ($0.1J' < kT < 0.2J'$) the main difference in the γ temperature dependence is a change from exponential (see Sec. III) to more power-law-like behavior. The linear part of the γ ($0.2J' < kT < 0.4J'$) resembles that found in Sec. III (compare Fig. 3 with Fig. 8). Moreover, comparing the specific heat for different parameters sets found in the Ising limit (Fig. 5) with the one ob-

$$\begin{aligned} \zeta_{\mathbf{k}}^1 &= (\cos \phi_{\mathbf{k}})d_{\mathbf{k}} - (\sin \phi_{\mathbf{k}})f_{\mathbf{k}}, \\ \zeta_{\mathbf{k}}^2 &= (\cos \phi_{\mathbf{k}})f_{\mathbf{k}} + (\sin \phi_{\mathbf{k}})d_{\mathbf{k}} \end{aligned} \quad (4.1)$$

and next the Bogoliubov transformations

$$\begin{aligned} \alpha_{\mathbf{k}} &= (\cosh \theta_{\mathbf{k}})\zeta_{\mathbf{k}}^1 - (\sinh \theta_{\mathbf{k}})\zeta_{-\mathbf{k}}^{2\dagger}, \\ \beta_{\mathbf{k}} &= (\cosh \theta_{\mathbf{k}})\zeta_{\mathbf{k}}^2 - (\sinh \theta_{\mathbf{k}})\zeta_{-\mathbf{k}}^{1\dagger}, \end{aligned} \quad (4.2)$$

which in the LSWA for $\tan(2\phi_{\mathbf{k}}) = JJ' \gamma_{\mathbf{k}} / \{\sqrt{2}[J^2(1-\gamma_{\mathbf{k}}^2) + JJ' + 3/16(J')^2]\}$ and $\tanh(2\theta_{\mathbf{k}}) = -(J+J'/4)\sin(2\phi_{\mathbf{k}})/J\gamma_{\mathbf{k}}$ give the Hamiltonian with independent $\alpha_{\mathbf{k}}$, $\beta_{\mathbf{k}}$, and $f'_{\mathbf{k}}$ modes. Performing two additional Bogoliubov transformations for $\alpha_{\mathbf{k}}$ and $\beta_{\mathbf{k}}$ states, we have found the magnon dispersions as presented in Fig. 6. The high-energy magnon branch [see Fig. 6(a)] has the energy gap $\Delta_d \approx 20.1, 44.8, 63.5$ for $J' = 1, 5, 10$ (with $J=100$), respectively. Thus, as in Sec. III, we have $\Delta_d \sim \sqrt{JJ'}$, which plays a leading role beyond the LSWA.

The 3D model is more complicated as both $f_{\mathbf{k}}$ and $f'_{\mathbf{k}}$ modes are involved [see Eq. (2.5)]. Therefore, to solve it numerically we have made the Bogoliubov transformation (3.1), which gives the H_{df} part of the Hamiltonian of the form

$$\begin{aligned} H_{df} &= A^{df} \sum_{\mathbf{k}} [(\alpha_{\mathbf{k}}^\dagger f_{-\mathbf{k}}^\dagger + \alpha_{\mathbf{k}} f_{-\mathbf{k}})u_{\mathbf{k}}\cos(k_z b) \\ &+ (\alpha_{\mathbf{k}}^\dagger f_{\mathbf{k}} + f_{\mathbf{k}}^\dagger \alpha_{\mathbf{k}})v_{\mathbf{k}}\cos(k_z b) \\ &+ (\alpha_{\mathbf{k}}^\dagger f'_{-\mathbf{k}} + \alpha_{\mathbf{k}} f'_{-\mathbf{k}})u_{\mathbf{k}}\sin(k_z b) \\ &+ (\alpha_{\mathbf{k}}^\dagger f'_{\mathbf{k}} + f'_{\mathbf{k}} \alpha_{\mathbf{k}})v_{\mathbf{k}}\sin(k_z b)]. \end{aligned} \quad (4.3)$$

Next we perform a simplifying approximation assuming $u_{\mathbf{k}}f_{-\mathbf{k}}^\dagger - v_{\mathbf{k}}f_{-\mathbf{k}} \approx 0$. Now the whole Hamiltonian can be easily diagonalized by a simple rotation of the $\alpha_{\mathbf{k}}, f_{\mathbf{k}}, f'_{\mathbf{k}}$ states, which leads to the calculation of eigenvalues of the matrix

interest here. At higher temperatures ($0.1J' < kT < 0.2J'$) the main difference in the γ temperature dependence is a change from exponential (see Sec. III) to more power-law-like behavior. The linear part of the γ ($0.2J' < kT < 0.4J'$) resembles that found in Sec. III (compare Fig. 3 with Fig. 8). Moreover, comparing the specific heat for different parameters sets found in the Ising limit (Fig. 5) with the one ob-

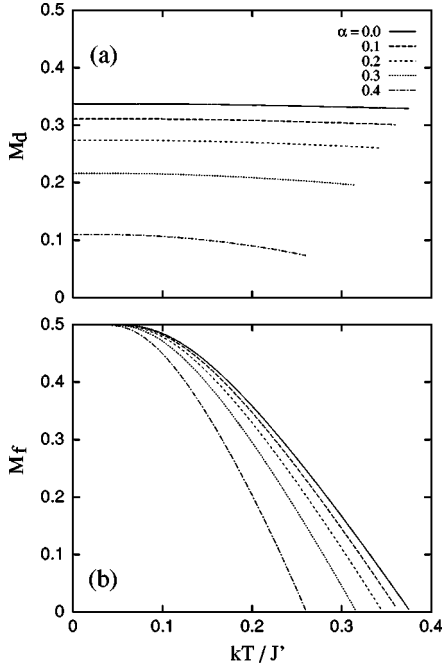


FIG. 4. Magnetic moments (in units of μ_B) of (a) Cu^{+3} and (b) Nd^{+3} ions as a function of temperature for different frustrations, calculated for realistic parameters of NCCO in the Ising limit $J'_\perp = 0$.

tained in this case, we have found only small quantitative differences. For these reasons, we argue that the anomaly in the γ coefficient is not connected with the \mathbf{k} -linear mode near the $(0,0,0)$ point, which was absent in Sec. III.

Using the analytical expression (2.8), one can obtain the Pauli-type susceptibility for different frustrations (see Fig. 9). At $T=0$ the value of χ_\perp steadily increases from $2.4(g\mu_B)^2$ to over $3.2(g\mu_B)^2$ for α increasing from 0 to 0.4. These results can be qualitatively understood as follows. When the parent compound is doped, the effective Cu-Cu superexchange interaction J is reduced on average due to the

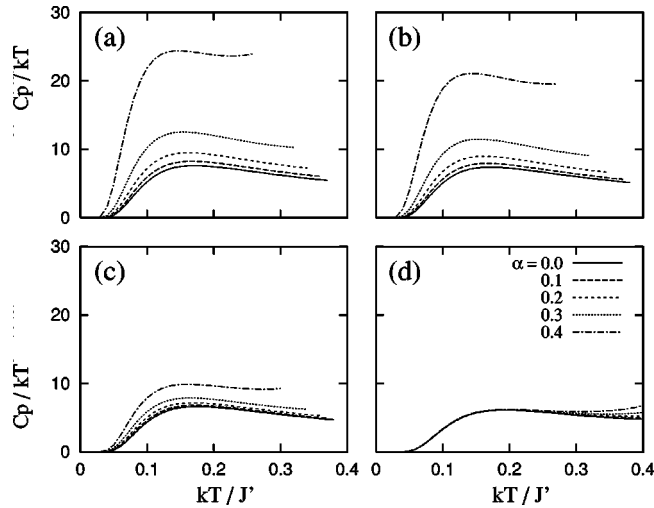


FIG. 5. Temperature dependence of the γ coefficient in the Ising limit $J'_\perp = 0$ including the magnon-magnon interactions for different frustrations, found for (a) $J/J' = 100$ and $J''/J' = 0.5$, (b) $J/J' = 100$ and $J''/J' = 1$, (c) $J/J' = 20$ and $J''/J' = 0.1$, and (d) $J/J' = 1$ and $J''/J' = 0.1$.

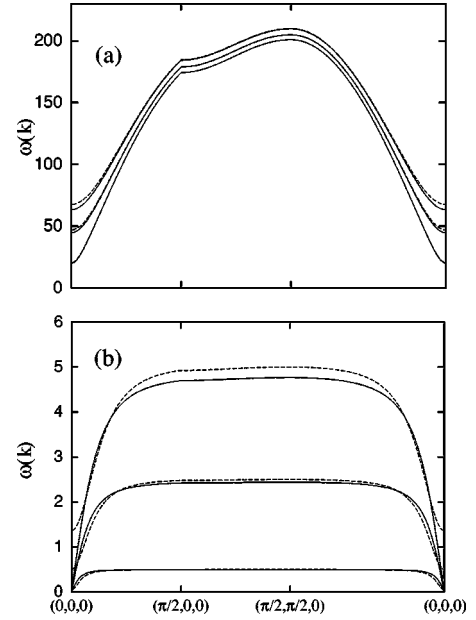


FIG. 6. Dispersions of (a) Cu and (b) Nd-like magnons in the 2D LSWA ($k_z=0$, $J''=0$) given by the exact solution (solid lines) and using the simplifying approximation (dashed lines). Magnons with increasing dispersions are obtained for $J/J' = 100$, $J/J' = 20$, and $J/J' = 10$, respectively. In all cases $J = 100$ and $\alpha = 0$.

presence of hole carriers. As a consequence, the susceptibility at zero temperature, being inversely proportional to the spin superexchange, should increase. In Table I we have put together values of the γ coefficient χ_\perp and the Sommerfeld-Wilson ratio $R = 4\pi^2 k_B^2 \chi / 3g^2 \mu_B^2 \gamma$ for frustration changing from $\alpha = 0.2$ to $\alpha = 0.42$. The increase in γ exceeds changes in χ_\perp leading to the Sommerfeld-Wilson ratio decreasing from 3.39 ($\alpha = 0$) to 1.04 ($\alpha = 0.42$).

Finally, we would like to make a more quantitative comparison of the value of specific heat with the experimental results. Assuming the energy of the Nd spin excitations $\omega_f \sim 0.8$ meV (Refs. 5, 12, and 38) at $kT = 0.2J'$, we have $\gamma \approx 2.7$ and 5.8 (J/mol K²) for $\alpha = 0.3$ and 0.4 , respectively. These results are the same order of magnitude as the experimental ones.¹

Another similarity of NCCO with heavy-fermion systems³⁹ is the influence of a magnetic field upon the γ coefficient. As presented in Fig. 10, the specific heat in our

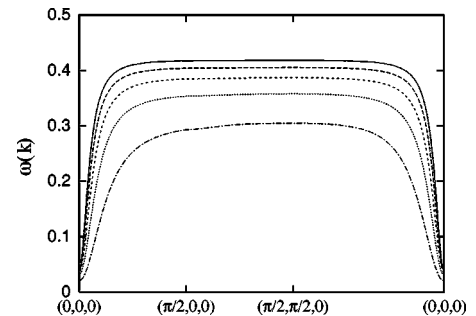


FIG. 7. Dispersions of Nd-like spin waves (only bonding mode) found in the Heisenberg limit $J'_\perp = J'_\parallel$ for the realistic parameters of NCCO at $T=0$. Magnons with decreasing dispersion are obtained for $\alpha = 0, 0.1, 0.2, 0.3$, and 0.4 , respectively.

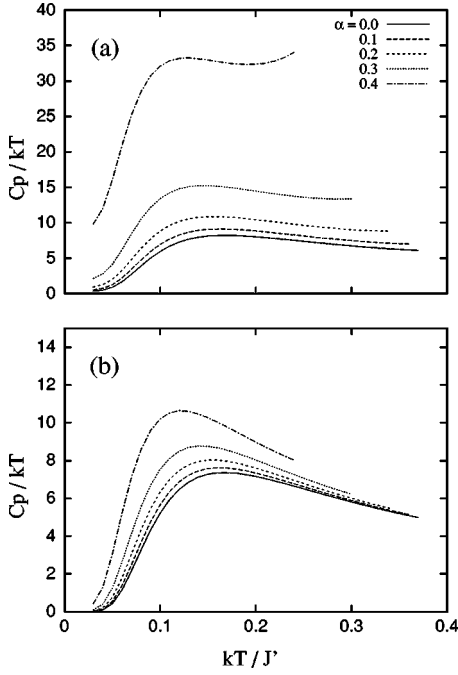


FIG. 8. Temperature dependence of the γ coefficient for different frustrations found in the Heisenberg limit $J'_\perp = J'_\parallel$ (a) with and (b) without magnon-magnon interactions and calculated for realistic parameters of NCCO.

model drops to much smaller values already at $h/g\mu_B \approx 0.2J'$, in agreement with the anomaly found experimentally.¹ This sets the characteristic energy scale for the interaction between an external field and Nd moments, which is the same as our temperature range where γ stabilizes at large values ($kT \sim 0.2J' - 0.4J'$).

V. SUMMARY

In this paper we have studied the physical properties of the 3D spin model with magnetic ions weakly coupled to strongly correlated electrons in CuO_2 planes. The spin dynamics was treated beyond the LSWA, producing qualitatively different results from those obtained using the LSWA or the low-temperature expansion (which can only reproduce the steep increase in the specific heat for $kT < 0.1J'$). The main limitation of this approach is the restriction to temperatures and doping where for both Cu and Nd moments LRO

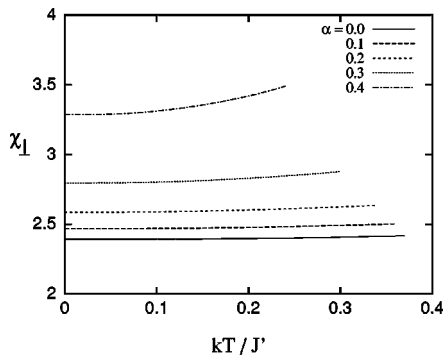


FIG. 9. Magnetic susceptibility [in units of $(g\mu_B)^2$] perpendicular to the quantization axis for realistic parameters of NCCO with different frustrations.

TABLE I. The γ coefficient, the magnetic susceptibility χ_\perp , and the Sommerfeld-Wilson ratio R for realistic parameters with different frustrations α at $kT = 0.2J'$.

α	γ	$\chi_\perp / (g\mu_B)^2$	$R = 4\pi^2 k_B^2 \chi / 3g^2 \mu_B^2 \gamma$
0.20	10.1	2.60	3.39
0.22	10.6	2.64	3.28
0.24	11.2	2.67	3.14
0.26	12.0	2.72	2.98
0.28	12.9	2.77	2.83
0.30	14.1	2.83	2.64
0.32	15.6	2.91	2.45
0.34	17.8	3.00	2.22
0.36	20.8	3.11	1.97
0.38	25.3	3.25	1.69
0.40	32.8	3.45	1.38
0.42	47.5	3.74	1.04

exist. Therefore, nothing can be said about the Schottky anomaly present above the Nd Néel temperature.^{10,40} The driving force of the phenomena presented here is magnon-magnon scattering, which, in a system with strongly correlated electrons, can dominate the specific heat at higher temperatures when AF order is sufficiently frustrated and consequently the Néel temperature sufficiently reduced. In NCCO the large γ onset is already in the Cu AF ordered phase ($0.1 < x < 0.14$) where γ reaches about 70% of its maximal value. Although our calculations cannot give a linear term in the $T=0$ limit they distinctly show that for $kT > 0.2J'$ the changes in the γ coefficient can be even quantitatively explained by our spin-only model when dynamical effects are taken into account. Moreover, as it has been presented in Sec. IV, the calculated values of γ and the γ/χ_\perp ratio are close to the experimental results in a doped compound.

Comparing the results in Secs. III and IV, we notice a minor role of the \mathbf{k} -linear mode near the $(0,0,0)$ point (see Fig. 7). The number of magnons n excited in this mode is $n \sim (T/J)^3$. Keeping T constant ($kT \sim J'$) and increasing J , we have $n \sim (J'/J)^3$ decreasing (the stronger correlated copper spins the steeper $\mathbf{k} \rightarrow 0$ mode). Thus, when $J \gg J'$ most of the excited states lie in the nondispersive part of the low-energy magnon branches, which are almost identical in both limits.

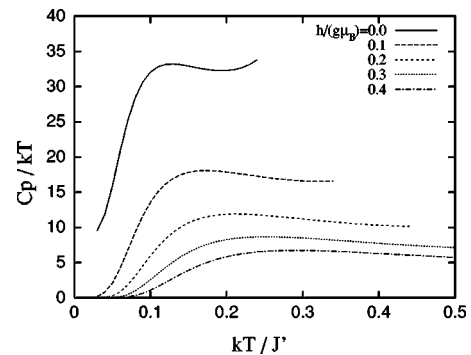


FIG. 10. Temperature dependence of the γ coefficient in the Heisenberg limit $J'_\perp = J'_\parallel$ for the realistic parameters of NCCO with $\alpha = 0.4$ and the magnetic field h parallel to the quantization axis.

Another issue, not considered in detail in this paper, is the role played by the direct Nd-Nd and Nd-Ce (in doped sample) exchange. In a doped compound Nd magnetic ions are substituted by nonmagnetic Ce^{4+} ones. This allows one to treat these interactions as frustrated (in a similar way to Cu-Cu ones). Numerical calculations show that these interactions only enlarge the Nd contribution to the specific heat but do not affect Cu-Nd magnon-magnon scatterings, which determine the character of the γ coefficient at larger values of α .

ACKNOWLEDGMENTS

This work was stimulated by intense discussions with Professor P. Fulde and Professor J. Igarashi. I wish to thank Professor A. M. Oleś for valuable advice concerning several aspects of this problem. I acknowledge the support of the MPI für Physik Komplexer Systeme, Dresden, where the main part of this work was performed. The financial support by the Committee of Scientific Research (KBN) of Poland, Project No. 2 P03B 175 14, is also acknowledged.

-
- ¹T. Brugger, T. Schreiner, G. Roth, P. Adelman, and G. Czjzek, *Phys. Rev. Lett.* **71**, 2481 (1993).
- ²H. Takagi, S. Uchida, and Y. Tokura, *Phys. Rev. Lett.* **62**, 1197 (1989); Y. Tokura, H. Takagi, and S. Uchida, *Nature (London)* **337**, 345 (1989); J. M. Tranquada, S. M. Heald, A. R. Moodenbaugh, G. Liang, and M. Craft, *ibid.* **337**, 720 (1989).
- ³M. Matsuda, K. Yamada, K. Kakurai, H. Kadowaki, T. R. Thurston, Y. Endoh, Y. Hidaka, R. J. Birgeneau, M. A. Kastner, P. M. Gehring, A. H. Moudden, and G. Shirane, *Phys. Rev. B* **42**, 10 098 (1990).
- ⁴S. B. Oseroff, D. Rao, F. Wright, D. C. Vier, S. Schultz, J. D. Thompson, Z. Fisk, S.-W. Cheong, M. F. Hundley, and M. Tovar, *Phys. Rev. B* **41**, 1934 (1990).
- ⁵M. Loewenhaupt, P. Fabi, S. Horn, P. v. Aken, and A. Severing, *J. Magn. Magn. Mater.* **140-144**, 1293 (1995).
- ⁶A. S. Ivanov, Ph. Bourges, D. Petitgrand, and J. Rossat-Mignod, *Physica B* **213-214**, 60 (1995).
- ⁷S. Skanthakumar, J. W. Lynn, J. L. Peng, and Z. Y. Li, *Phys. Rev. B* **47**, 6173 (1993).
- ⁸P. Fulde, V. Zevin, and G. Zwicknagl, *Z. Phys. B* **92**, 133 (1993).
- ⁹J. Igarashi, T. Tonegawa, M. Kaburagi, and P. Fulde, *Phys. Rev. B* **51**, 5814 (1995).
- ¹⁰J. Igarashi, K. Murayama, and P. Fulde, *Phys. Rev. B* **52**, 15 966 (1995).
- ¹¹W. Henggeler, T. Chattopadhyay, B. Roessli, P. Vorderwisch, P. Thalmeier, D. I. Zhigunov, S. N. Barilo, and A. Furrer, *Phys. Rev. B* **55**, 1269 (1997).
- ¹²P. Thalmeier, *Physica C* **266**, 89 (1996).
- ¹³W. Zhang, J. Igarashi, and P. Fulde, *Phys. Rev. B* **56**, 654 (1997).
- ¹⁴S. Skanthakumar, J. W. Lynn, J. L. Peng, and Z. Y. Li, *J. Magn. Magn. Mater.* **104-107**, 519 (1992).
- ¹⁵J. Zaanen and A. M. Oleś, *Phys. Rev. B* **37**, 9423 (1988); P. Prelovšek, *Phys. Lett. A* **126**, 287 (1988).
- ¹⁶M. Inui, S. Doniach, and M. Gabay, *Phys. Rev. B* **38**, 6631 (1988); T. Tohyama and S. Maekawa, *ibid.* **49**, 3596 (1994); R. J. Gooding, K. J. E. Vos, and P. W. Leung, *ibid.* **50**, 12 866 (1994); J. F. Annett, R. Martin, A. McMahan, and S. Satpathy, *ibid.* **40**, 2620 (1989); D. Ihle and M. Kasner, *ibid.* **42**, 4760 (1990); A. Chubukov, E. Gagliano, and C. Balseiro, *ibid.* **45**, 7889 (1992); J. Bala and A. M. Oleś, *ibid.* **54**, 3495 (1996); H. J. Schmidt and Y. Kuramoto, *Physica C* **167**, 263 (1990).
- ¹⁷F. Nori, E. Gagliano, and S. Bacci, *Phys. Rev. Lett.* **68**, 240 (1992).
- ¹⁸S. Ghamaty, B. W. Lee, J. T. Markert, E. A. Early, T. Bjornholm, C. L. Seaman, and M. B. Maple, *Physica C* **160**, 217 (1989).
- ¹⁹N. D. Mermin and H. Wagner, *Phys. Rev. Lett.* **17**, 1133 (1966).
- ²⁰J. E. Hirsch and S. Tang, *Phys. Rev. B* **39**, 2887 (1989); E. Dagotto and A. Moreo, *Phys. Rev. Lett.* **63**, 2148 (1989).
- ²¹H. J. Schulz and T. A. L. Ziman, *Europhys. Lett.* **18**, 355 (1992).
- ²²J. Richter, *Phys. Rev. B* **47**, 5794 (1993).
- ²³P. Chandra and B. Doucot, *Phys. Rev. B* **38**, 9335 (1988).
- ²⁴A. V. Chubukov, Th. Jolicoeur, *Phys. Rev. B* **44**, 12 050 (1991).
- ²⁵C. Bruder and F. Mila, *Europhys. Lett.* **17**, 463 (1992).
- ²⁶N. Read and S. Sachdev, *Phys. Rev. Lett.* **66**, 1773 (1991).
- ²⁷H. Nishimori and Y. Saika, *J. Phys. Soc. Jpn.* **59**, 4454 (1990); J. H. Xu and C. S. Ting, *Phys. Rev. B* **42**, 6861 (1990).
- ²⁸F. Mila, D. Poilblanc, and C. Bruder, *Phys. Rev. B* **43**, 7891 (1991).
- ²⁹J. Ferrer, *Phys. Rev. B* **47**, 8769 (1993); P. Simon, *ibid.* **56**, 10 975 (1997).
- ³⁰J. Richter, *Phys. Lett. A* **140**, 81 (1989); F. Figueirido, A. Karlhede, S. Kivelson, S. Sondhi, M. Rocek, and D. S. Rokhsar, *Phys. Rev. B* **41**, 4619 (1990); J. Richter, *Z. Phys. B* **80**, 403 (1990).
- ³¹R. R. P. Singh and R. Narayanan, *Phys. Rev. Lett.* **65**, 1072 (1990).
- ³²V. Kalmeyer and R. B. Laughlin, *Phys. Rev. Lett.* **59**, 2095 (1987); X. G. Wen, F. Wilczek, and A. Zee, *Phys. Rev. B* **39**, 11 413 (1989); J. Richter, C. Gross, and W. Weber, *ibid.* **44**, 906 (1991).
- ³³D. C. Mattis, in *The Theory of Magnetism I*, edited by P. Fulde, Springer Series in Solid-State Physics Vol. 17 (Springer, Berlin, 1981).
- ³⁴R. Kubo, *Phys. Rev.* **87**, 568 (1952).
- ³⁵J. W. Lynn, I. W. Sumarlin, S. Skanthakumar, W.-H. Li, R. N. Shelton, J. L. Peng, Z. Fisk, and S.-W. Cheong, *Phys. Rev. B* **41**, 2569 (1990).
- ³⁶I. W. Sumarlin, J. W. Lynn, T. Chattopadhyay, S. N. Barilo, D. I. Zhigunov, and J. L. Peng, *Phys. Rev. B* **51**, 5824 (1995).
- ³⁷V. L. Sobolev, H. L. Huang, Yu. G. Pashkevich, M. M. Larionov, I. M. Vitebsky, and V. A. Blinkin, *Phys. Rev. B* **49**, 1170 (1994).
- ³⁸A. T. Boothroyd, S. M. Doyle, D. M. Paul, and R. Osborn, *Phys. Rev. B* **45**, 10 075 (1992); A. T. Boothroyd, S. M. Doyle, D. M. K. Paul, and D. S. Misra, *Physica C* **165**, 17 (1990).
- ³⁹C. D. Bredl, S. Horn, F. Steglich, B. Lüthi, and R. M. Martin, *Phys. Rev. Lett.* **52**, 1982 (1984).
- ⁴⁰P. Adelman, R. Ahrens, G. Czjzek, G. Roth, H. Schmidt, and C. Steinleitner, *Phys. Rev. B* **46**, 3619 (1992).